

K. U. Anderson

No. 1323

# NATIONAL ADVISORY COMMITTEE FOR AERONAUTICS

TECHNICAL NOTE

No. 1323

CHARTS FOR THE MINIMUM-WEIGHT DESIGN  
OF MULTIWEB WINGS IN BENDING

By Evan H. Schuette and James C. McCulloch

Langley Memorial Aeronautical Laboratory  
Langley Field, Va.

**LIBRARY COPY**

PR 2 : 1993



LANGLEY RESEARCH CENTER  
LIBRARY NASA  
HAMPTON, VIRGINIA

Washington

June 1947

**FOR REFERENCE**

NOT TO BE TAKEN FROM THIS ROOM



## NATIONAL ADVISORY COMMITTEE FOR AERONAUTICS

TECHNICAL NOTE NO. 1323

CHARTS FOR THE MINIMUM-WEIGHT DESIGN  
OF MULTIWEB WINGS IN BENDING

By Evan H. Schuette and James C. McCulloch

## SUMMARY

A method for the calculation of the buckling stress of a multiweb wing in bending is presented, and design charts based on this method are developed for the minimum-weight design of multiweb wings of 24S-T aluminum-alloy sheet, extruded 75S-T aluminum alloy, and extruded O-1HTA magnesium alloy. These charts make possible the design of the lightest wings of this type for a wide range of design requirements. An example of the use of the charts is given.

## INTRODUCTION

Because of the small absolute depth of thin high-speed wings, some designers are considering the use of a type of construction that employs a number of shear webs with no intermediate stiffening of the skin (multiweb wing). For a wing of this type, as for any high-speed wing, the requirements of a smooth surface or a high torsional stiffness result in the use of a fairly thick skin. If the aspect ratio of the wing is relatively low, the compressive stresses due to bending of the wing may be low and the problem of buckling, therefore, a minor one. If the aspect ratio is relatively high, however, the buckling of the structure due to bending may be of primary significance, in spite of the relatively thick skin.

The present report considers a multiweb wing in which the buckling of the webs and compression skin under bending loads is of primary significance in the design. A method for calculating the buckling stress is provided and design charts are presented from which the proportions for minimum weight can be chosen. An example of the use of the design charts is given.

The methods by which the various charts were prepared are discussed in appendixes A and B. Appendix C gives a discussion of the effects of shear in the webs.

## SYMBOLS

- $A_1$  area per chordwise inch of web and compression skin, inches
- $D$  plate stiffness in bending, inch-kips  $\left( \frac{Et^3}{12(1-\mu^2)} \right)$
- $E$  Young's modulus of elasticity, ksi
- $M_i$  moment per chordwise inch, inch-kips per inch
- $N_o$  intensity of compressive force in x direction at edge of plate  $y = 0$ , kips per inch
- $N_x$  intensity of distributed forces in x direction at edges of plate  $x = 0$  and  $x = \lambda$ , kips per inch
- $S_o$  stiffness per unit length of elastic restraining medium or amplitude of sinusoidally applied moment divided by amplitude of resulting sinusoidal rotation of elastic medium in quarter radians
- $S^{II}$  stiffness in moment-distribution analysis for far edge supported with no restraint against rotation
- $S^{IV}$  stiffness in moment-distribution analysis for far edge supported and subjected to sinusoidally distributed moment equal and opposite to moment applied at near edge
- $T$  external work of applied stress
- $V$  internal energy of deformation
- $a_1, a_n$  Fourier coefficients of  $\sin \frac{n\pi y}{b_w}$
- $b$  width of plate element, inches
- $i, j, n$  integers
- $k$  nondimensional critical-stress coefficient for plate-buckling formula
- $t$  thickness of plate element, inches

- w plate-buckling deformation, normal to plane of the plate
- x plate coordinate in direction of stress
- y plate coordinate, perpendicular to direction of stress
- $\beta$  ratio of half-wave length to plate width  $\left(\frac{\lambda}{b}\right)$
- $\gamma$  Lagrangian multiplier
- $\eta$  nondimensional coefficient that takes into account reduction of modulus of elasticity for stresses above the elastic range; within the elastic range,  $\eta = 1$
- $\mu$  Poisson's ratio
- $\lambda$  half-wave length of buckles in longitudinal direction, inches
- $\epsilon$  nondimensional restraint coefficient given by the formula  $\left(\frac{4S_0b}{D}\right)$
- $\sigma$  longitudinal compressive stress, ksi
- $\tau$  shear stress, ksi
- $R_s$  ratio of shear stress  $\tau$  actually present to critical shear stress  $\tau_{cr}$  when no other stresses are present
- $R_b$  ratio of bending stress  $\sigma$  actually present to critical bending stress  $\sigma_{cr}$  when no other stresses are present
- $\theta$  amplitude of sinusoidal edge rotation

## Subscripts:

- p referring to plate
- r referring to restraint
- S skin
- W web
- cr critical

cy compressive yield  
max maximum  
eq equivalent

## BUCKLING STRESS OF A MULTIWEB WING

### Simplifying Assumptions

For purposes of analysis, the multiweb wing has been idealized to an infinitely wide, infinitely long, integral flat-plate structure of the type indicated in figure 1. A discussion of the effect of each of the simplifying assumptions employed follows:

Infinite width.- For a wing with four or more shear webs, the error made in assuming infinite width should be quite small.

Infinite length.- The assumption that the wing is infinitely long may be considered conservative because the insertion of uprights on the webs, or of bulkheads or ribs, would tend to force the buckling into wave lengths other than its natural wave length and thus to raise the buckling stress. The amount of conservatism, however, is probably quite small for normal spacing of uprights, bulkheads, or ribs.

Integral nature of assumed structure.- No published data are available to indicate the effect of riveted or otherwise assembled joints in altering the buckling stress from that for an integral (or continuous) structure. The effect would depend greatly on the design of the attachment. Observations made in the course of other research programs have indicated that the effect is probably quite small for conservatively designed conventional attachments.

Flat compression skin.- The assumption of a flat compression skin is conservative, as the introduction of curvature would tend to increase the buckling stress. Again, however, the amount of conservatism is probably small, because the multiweb construction is most applicable to very thin wings, where the deviation from flatness in the region between webs is quite small.

Simple support at lower edge of webs.- Because the tension skin will always provide a finite amount of restraint against web buckling, the replacement of the tension skin by a simple support is conservative. For one check case discussed in appendix A, however, it was

found that an increase of the restraint at the lower edge of the web all the way from simple support to complete fixity produced an increase of only 0.8 percent in the buckling stress.

Symmetrical bending. - In the analysis, the neutral axis was assumed to be at the center of the web. Whether this assumption is valid for a particular wing depends upon the relative thicknesses of tension and compression skins and upon the symmetry or asymmetry of the airfoil section. If skin thicknesses are dictated by torsional stiffness and if camber is small - both conditions being likely in very thin wings - the assumption of symmetrical bending should not represent a very severe departure from the actual conditions.

Pure bending. - In the calculation of the buckling loads and the preparation of the design charts, the wing is assumed to be subjected to pure bending and the effects of shear, torsion, and local air loads are neglected. If the aspect ratio of the wing is high the buckling of the structure due to bending may be of primary significance. Even if the aspect ratio is high, however, there may be sufficient shear on the wing to preclude the assumption of pure bending (zero shear in the webs). An evaluation of this assumption is made in appendix C.

#### Charts for Calculation of Buckling Stress

The chart for calculation of the buckling stress of a multiweb wing, based on the preceding simplifications, is given in figure 2. The method of preparation of this chart is discussed in appendix A. This chart is of a type similar to those given in reference 1 for columns of I-, Z-, channel-, and rectangular-tube section, and those given in reference 2 for web- and T-stiffened compression panels.

The elastic stress  $\frac{\sigma_{cr}}{\eta}$  in the compression surface at which buckling takes place is given by the formula

$$\frac{\sigma_{cr}}{\eta} = \frac{k_S \pi^2 E t_S^2}{12 (1 - \mu^2) b_S^2} \quad (1)$$

The value of  $k_S$  for any given set of dimension ratios is picked from figure 2, and the values of  $E$  and  $\mu$  are for the material being considered.

The value of  $\sigma_{cr}$ , probably conservative, can be obtained, once  $\sigma_{cr}/\eta$  is known, from the curves for various aircraft structural materials given in references 3 to 9, and the value of  $\bar{\sigma}_{max}$  can be estimated from these same references.

## DESIGN CHARTS

### Discussion of Charts

Design charts for multiweb wings, based on buckling stresses obtained from figure 2 and experimental data from references 3, 5, and 9, are given in figures 3 to 6. The method by which the design charts are prepared is outlined in appendix B. Charts are presented for 24S-T aluminum-alloy sheet, extruded 75S-T aluminum alloy, and extruded O-LHTA magnesium alloy. A second chart for O-LHTA which makes possible direct comparison with the other two materials is also presented. Lack of experimental data at the present time prevents the preparation of charts for a high-strength aluminum-alloy sheet material or for magnesium-alloy sheet. It has been assumed in the preparation of the charts that one of the design requirements for a multiweb wing is that buckling shall not be permitted under any flight condition. The value of  $\bar{\sigma}_{max}$  used in the preparation of the charts was consequently never allowed to exceed  $1.5\sigma_{cr}$ .

The quantities with which the charts are entered are  $b_w/t_s$  (the ratio of depth to skin thickness for the wing) and  $M_1/b_w t_s$ , which defines the loading condition. (The quantity  $M_1/b_w t_s$  represents the highest stress attainable, as it is the stress that would be developed were the entire load carried in the skin alone.) The quantities to be read from the charts are the dimension ratios  $t_w/t_s$  and  $b_w/t_s$  and the efficiency parameter  $M_1/b_w A_1$ . If  $M_1$  and  $b_w$  are fixed, the value of  $M_1/b_w A_1$  is an inverse measure of the area (and thus also of the weight) of the resulting design. The higher the value of  $M_1/b_w A_1$ , the less the weight and the greater the efficiency of the structure.

If two materials of different densities are being considered, the comparative values of  $M_1/b_w A_1$  for the two materials provide an inverse measure of the comparative areas but not of the

comparative weights. In order to make possible direct weight comparisons between aluminum and extruded O-1HTA magnesium alloy, figure 6 has been prepared, in which the value of  $A_1$  has been replaced by  $A_{1eq}$ , the area per inch of an aluminum structure of the same weight as the magnesium structure. Similarly,  $M_1/b_W t_S$  and  $b_W/t_S$  are replaced by ratios based on equivalent thicknesses of aluminum,  $M_1/b_W t_{Seq}$  and  $b_W/t_{Seq}$ .

Example of Use of a Design Chart

The procedure in using the design charts can best be illustrated by carrying through a sample design. Suppose the value of  $M_1$  is 300 inch-kips per inch and the wing depth  $b_W$  is 15 inches. For comparative purposes, 24S-T aluminum-alloy designs will be made for values of skin thickness  $t_S$  of 0.4, 0.5, and 0.6 inch. The procedure is then as outlined in the following table:

(1)	(2)	(3)	(4)	(5)	(6)	(7)	(8)	(9)	(10)	(11)
$t_S$ (in)	$\frac{M_1}{b_W t_S}$	$\frac{b_W}{t_S}$	$\frac{t_W}{t_S}$	$\frac{b_W}{b_S}$	$\frac{M_1}{b_W A_1}$	$t_W$ (in)	$b_S$ (in)	$A_1$ (in)	$A_1+t_S$ (in)	Weight (lb/sq ft)
			from fig. 3			(1)×(4)	$\frac{15}{(5)}$	$\frac{300}{15 \times (6)}$	(1)+(9)	14.4×(10)
0.4	50.00	37.50	0.453	1.497	29.9	0.181	10.02	0.669	1.069	15.4
.5	40.00	30.00	.305	1.000	30.7	.152	15.00	.652	1.152	16.6
.6	33.33	25.00	.225	.737	28.6	.135	20.36	.699	1.299	18.7

Because the value of  $A_1$  includes only the compression skin and webs, the thickness of the tension skin is added (column (10)) before the structural weight of the wing is computed. This structural weight of the wing is, of course, a minimum value, which would be increased by the weight of any attachments and fittings required.

The three designs arrived at in the foregoing table are illustrated in figure 7. These designs might be called the ideal configurations. They would undoubtedly have to be adjusted in any

given case to make use of available sheet gages and to provide an integral number of sheet bays across the width of the wing. Such adjustments must naturally depend on the particular circumstances in each design. After the adjustment is made, the safety of the final design can be estimated through figure 2 and the appropriate curve of  $\sigma_{\max}$  against  $\sigma_{cr}/\eta$  from references 3 to 9.

It should not be concluded from the example that a thicker skin always results in a greater wing weight, because for some dimension ratios a slightly lighter design was found to be obtained by using a thicker skin.

Langley Memorial Aeronautical Laboratory  
National Advisory Committee for Aeronautics  
Langley Field, Va., April 1, 1947

## APPENDIX A

## PREPARATION OF CHART FOR CALCULATION OF BUCKLING STRESS

## Summary of Procedure

The preparation of the chart for the calculation of the buckling stress of a multiweb wing was accomplished in two steps. First, a calculation was carried through and a chart prepared for obtaining the buckling stress of a plate undergoing bending in the plane of the plate, with the tension edge simply supported and the compression edge subjected to various degrees of elastic restraint. Second, the interaction of such a plate and the compression skin was considered and from these considerations the chart of figure 2 was prepared.

## Buckling Stress of a Plate in Bending

For the calculation of the critical stress of an infinitely long flat plate under bending forces in the plane of the plate the energy method was used. The plate is simply supported along the tension edge and subjected to various degrees of elastic restraint along the compression edge. The elastic restraint is assumed to arise from an elastic medium distributed along the compression edge; this elastic medium has the basic property that a sinusoidally applied moment causes a sinusoidal rotation in phase with the moment. Thus, this elastic medium is equivalent to the compression skin when the wave lengths of the medium and the compression skin are equal. The critical stress of the plate is obtained from the condition of neutral stability in which the work done by external forces must equal the strain energy of the buckled plate plus the energy of the restraining medium.

Figure 8 shows the coordinate system and the plate dimensions. The intensity of the distributed forces acting in the middle plane of the plate is given by the equation

$$N_x = N_0 \left( 1 - 2 \frac{y}{b_w} \right) \quad (A1)$$

The deflection surface of the buckled plate can be represented by the series

$$w = \sin \frac{\pi x}{\lambda_w} \sum_{n=1}^{\infty} a_n \sin \frac{n\pi y}{b_w} \quad (A2)$$

Substitution of equation (A2) in the expression for the strain energy of bending (for this case equation 199, reference 10) gives

$$V_p = \frac{D_W \lambda_W b_W \pi^4}{8} \sum_{n=1}^{\infty} a_n^2 \left( \frac{1}{\lambda_W^2} + \frac{n^2}{b_W^2} \right) \quad (A3)$$

where  $V_p$  is the strain energy of the buckled plate per half wave. The expression for the energy of the restraining medium per half wave is

$$V_r = S_o \theta^2 \lambda_W \quad (A4)$$

where  $\theta$  is the amplitude of the sinusoidal edge rotation and is given by

$$\theta = \sum_{n=1}^{\infty} a_n \frac{n\pi}{b_W} \quad (A5)$$

Substitution of equation (A2) in the expression for the work done by external forces on the plate (for this case equation 201, reference 10) gives

$$T = \frac{2N_o b_W}{\lambda_W} \sum_{n=1}^{\infty} \sum_{i=1}^{\infty} \frac{a_n a_i n i}{(n^2 - i^2)^2} \quad (A6)$$

( $n \pm i$  must be odd)

where  $T$  is the work done by the tensile and compressive forces during buckling. Equating this work to the strain energy of bending plus the energy of the restraining medium and making the substitutions

$$N_o = k_W \frac{\pi^2 D_W}{b_W^2}$$

$$S_o = \frac{D_W \epsilon}{4b_W}$$

$$\beta = \frac{\lambda_W}{b_W}$$

gives the following expression in  $k_W$

$$\sum_{n=1}^{\infty} a_n^2 (1 + \beta^2 n^2)^2 + 2\epsilon\theta^2 \beta^4 \frac{b_W^2}{\pi^4} = \frac{16\beta^2 k_W}{\pi^2} \sum_{n=1}^{\infty} \sum_{i=1}^{\infty} \frac{a_n a_i n i}{(n^2 - i^2)^2} \quad (A7)$$

( $n \pm i$  must be odd)

The coefficients  $a_n$  must be so adjusted as to make the expression for  $k_W$  a minimum with the constraining relationship that

$$\theta = \sum_{n=1}^{\infty} a_n \frac{n\pi}{b_W} \quad (A8)$$

This result is accomplished by means of the Lagrangian multiplier method outlined in reference 11. The expression to be minimized is

$$\sum_{n=1}^{\infty} a_n^2 (1 + \beta^2 n^2)^2 + 2\epsilon\theta^2 \beta^4 \frac{b_W^2}{\pi^4} - \frac{16\beta^2 k_W}{\pi^2} \sum_{n=1}^{\infty} \sum_{i=1}^{\infty} \frac{a_n a_i n i}{(n^2 - i^2)^2} - \gamma \left( \theta - \sum_{n=1}^{\infty} a_n \frac{n\pi}{b_W} \right) = 0 \quad (A9)$$

( $n \pm i$  must be odd)

with the constraining relationships (A8) when  $\gamma$  is the undetermined Lagrangian multiplier. Taking derivatives of this expression with respect to  $\theta$  and the coefficients  $a_n$ , equating these derivatives to zero, and simplifying gives the following set of linear homogeneous equations:

$$\left. \begin{aligned}
 a_n (1 + \beta^2 n^2)^2 - \frac{16\beta^2 k_W}{\pi^2} \sum_1^{\infty} \frac{a_1 n i}{(n^2 - i^2)^2} + \frac{\gamma n \pi}{2b_W} = 0 \\
 (n \pm i \text{ must be odd}) \\
 4\epsilon b_W \frac{\beta^4}{\pi^3} \sum_{n=1}^{\infty} a_n n - \gamma = 0
 \end{aligned} \right\} \text{(A10)}$$

For the purpose of these calculations it is considered sufficiently accurate to set

$$a_{j+8} = 0$$

where  $j = 0, 2, 4, \dots, \infty$ . Then,

$$a_1 = \frac{16\beta^2 k_W i}{\pi^2 (1 + \beta^2 i^2)^2} \left[ \frac{2a_2}{(i^2 - 4)^2} + \frac{4a_4}{(i^2 - 16)^2} + \frac{6a_6}{(i^2 - 36)^2} \right] - \frac{\gamma i \pi}{2b_W (1 + \beta^2 i^2)^2}$$

( $i = 1, 3, 5, \dots, \infty$ )

Substituting this equation into the equations (A10) gives the following set of stability equations:

$$\begin{aligned}
 a_n(1 + \beta^2 n^2)^2 &- \frac{256\beta^4 k_W^2 n}{\pi^4} \sum_{i=1,3,5,\dots}^{\infty} \frac{2i^2}{(n^2 - i^2)^2 (1 + \beta^2 i^2)^2 (i^2 - 4)^2} a_2 \\
 &- \frac{256\beta^4 k_W^2 n}{\pi^4} \sum_{i=1,3,5,\dots}^{\infty} \frac{4i^2}{(n^2 - i^2)^2 (1 + \beta^2 i^2)^2 (i^2 - 16)^2} a_4 \\
 &- \frac{256\beta^4 k_W^2 n}{\pi^4} \sum_{i=1,3,5,\dots}^{\infty} \frac{6i^2}{(n^2 - i^2)^2 (1 + \beta^2 i^2)^2 (i^2 - 36)^2} a_6 \\
 &+ \frac{n\pi}{2} \left[ 1 + \frac{16\beta^2 k_W}{\pi^2} \sum_{i=1,3,5,\dots}^{\infty} \frac{i^2}{(n^2 - i^2)^2 (1 + \beta^2 i^2)^2} \right] \frac{\gamma}{b_W} = 0
 \end{aligned}$$

$$\begin{aligned}
 &8 \frac{\beta^4}{\pi^3} \left[ 1 + \frac{16\beta^2 k_W}{\pi^2} \sum_{i=1,3,5,\dots}^{\infty} \frac{i^2}{(1 + \beta^2 i^2)^2 (i^2 - 4)^2} \right] a_2 \\
 &+ 16 \frac{\beta^4}{\pi^3} \left[ 1 + \frac{16\beta^2 k_W}{\pi^2} \sum_{i=1,3,5,\dots}^{\infty} \frac{i^2}{(1 + \beta^2 i^2)^2 (i^2 - 16)^2} \right] a_4 \\
 &+ 24 \frac{\beta^4}{\pi^3} \left[ 1 + \frac{16\beta^2 k_W}{\pi^2} \sum_{i=1,3,5,\dots}^{\infty} \frac{i^2}{(1 + \beta^2 i^2)^2 (i^2 - 36)^2} \right] a_6 \\
 &- \left[ \frac{1}{\epsilon} + 2 \frac{\beta^4}{\pi^2} \sum_{i=1,3,5,\dots}^{\infty} \frac{i^2}{(1 + \beta^2 i^2)^2} \right] \frac{\gamma}{b_W} = 0
 \end{aligned}
 \tag{A11}$$

In order that equations (All) be compatible, the determinant of the coefficients must vanish. The lowest value of  $k_W$  for which this determinant vanished is the desired buckling-stress coefficient.

Figure 9 shows a chart calculated from equations (All) with values of  $k_W$  plotted against  $\lambda_W/b_W$  for various values of a parameter  $\epsilon$ , termed the "restraint coefficient" along the compression edge. The restraint coefficient  $\epsilon$  is given by the expression

$$\epsilon = \frac{4S_0 b_W}{D_W} \quad (A12)$$

for the type of restraining medium in which a sinusoidally applied moment causes a sinusoidal rotation. With the coefficient  $k_W$  known, the elastic buckling stress  $\sigma_{cr}/\eta$  can be calculated from the expression

$$\frac{\sigma_{cr}}{\eta} = k_W \frac{\pi^2 D_W}{b_W^2 t_W} \quad (A13)$$

For the special case of elastic restraint along the tension edge with the compression edge simply supported, the same equations can be used as for elastic restraint along the compression edge. It is only necessary to obtain negative values of  $k_W$  from equations (All). The minimum negative value of  $k_W$  for the restraint coefficient  $\epsilon = \infty$  (complete fixity along the tension edge) was calculated and was found to differ from that for  $\epsilon = 0$  (simple support along the tension edge) by only 0.8 percent. Thus, in this case the assumption of simple support at the lower edge of the webs is conservative by only approximately 0.8 percent.

### Buckling Stress of a Multiweb Wing

The buckling stress of a multiweb wing was calculated by an application of the principles of moment distribution to the stability of thin plates. This method is presented in reference 12. For a structure composed of long plates under longitudinal load the condition of neutral stability gives the critical buckling stress for the structure and is obtained by setting the sum of the stiffnesses

of the members of any joint equal to zero. If the joint is assumed to be the intersection line between a web element and the compression skin, the total stiffness of the joint must be zero:

$$2S_S^{IV} + S_W^{II} = 0 \quad (A14)$$

Also, for equilibrium of the web, the restraint offered to the web must equal the negative of the stiffness of the web:

$$\frac{\epsilon \left( \frac{D}{b} \right)_W}{4} = -S_W^{II} \quad (A15)$$

Substituting equation (A15) in equation (A14) and simplifying in order to obtain the stiffness of the compression skin in terms of the restraint offered to the web gives

$$\frac{S_S^{IV}}{\left( \frac{D}{b} \right)_S} = \epsilon \frac{\left( \frac{t_W}{t_S} \right)^3}{8 \left( \frac{b_W}{b_S} \right)} \quad (A16)$$

As the stress in the web at the joint must equal the stress in the skin at the joint for equilibrium,

$$\sigma_W = \sigma_S$$

or

$$k_W \pi^2 \left( \frac{D}{b^2 t} \right)_W = k_S \pi^2 \left( \frac{D}{b^2 t} \right)_S$$

$$k_W = k_S \frac{\left( \frac{b_W}{b_S} \right)^2}{\left( \frac{t_W}{t_S} \right)^2} \quad (A17)$$

It is also necessary that the half-wave length of the web equal the half-wave length of the skin

$$\lambda_W = \lambda_S$$

or

$$\frac{\lambda_W}{b_W} = \frac{\lambda_S}{b_S} \quad (A18)$$

The critical buckling stress of the multiweb wing is, therefore, the lowest stress that satisfies the three conditions (equations (A16), (A17), and (A18)) simultaneously. The buckling coefficient  $k_S$  is determined by trial calculations and interpolation so that these conditions are met. The stiffness of the compression skin for different values of the parameter  $\lambda_S$  and  $k_S$  was obtained from the stiffness tables of reference 13. The stiffness of the web for different values of the parameter  $\lambda_S$  and  $k_S$  was obtained from figure 9 herein.

From these calculations the chart of figure 2 was constructed with values of  $k_S$  plotted against various dimension ratios of  $t_W/t_S$  and  $b_W/b_S$ . When the buckling coefficient  $k_S$  is known, the elastic critical stress for the multiweb wing can be calculated from the equation

$$\frac{\sigma_{cr}}{\eta} = k_S \pi^2 \left( \frac{D}{b^2 t} \right)_S \quad (A19)$$

## APPENDIX B

## DESIGN CHARTS

## Selection of Parameters

In order to prepare design charts, it is necessary to know what factors must be considered design conditions and what factors can be varied at the will of the designer. In order that the chart for each material may be completely general, it is also desirable that the parameters selected be either dimensionless or in units of stress.

For the design of a multiweb wing, the more important fixed conditions to be met are usually the moment per chordwise inch, the depth of the wing cross section, and the skin thickness. These design conditions can be specified in terms of the two parameters  $M_1/b_W t_S$  and  $b_W/t_S$ . The quantity  $M_1/b_W t_S$  represents the highest stress attainable, as it is the stress that would be developed were the entire load carried in the skin alone. The quantity  $b_W/t_S$  is simply the ratio of depth to skin thickness for the wing.

The thickness and spacing of the shear webs can be varied to produce the required strength. These quantities can be expressed in terms of the ratios  $t_W/t_S$  and  $b_W/b_S$ .

It is also desirable to have a parameter that gives a measure of the structural efficiency of the design. Such a quantity is  $M_1/b_W A_1$ . With  $M_1$  and  $b_W$  fixed, this quantity is an inverse measure of the area and thus, for given density, also an inverse measure of the weight of the compression skin and webs.

## Preparation of Design Charts

The procedure in preparing the charts is essentially one of working backward from certain proportions of the wing to the design conditions for which these proportions provide the most efficient cross section. The starting conditions are taken as values of  $M_1/b_W t_S$ ,  $t_W/t_S$ , and  $b_W/b_S$ . The other necessary quantities will now be evaluated in terms of these fixed values.

The area per chordwise inch of compression skin and webs is given by the area included in one bay divided by the width of that bay:

$$\begin{aligned} A_1 &= \frac{b_S t_S + b_W t_W}{b_S} \\ &= t_S + t_W \frac{b_W}{b_S} \end{aligned}$$

and

$$\frac{A_1}{t_S} = 1 + \frac{t_W}{t_S} \frac{b_W}{b_S} \quad (B1)$$

The value of  $M_1 / b_W A_1$  is then given by

$$\begin{aligned} \frac{M_1}{b_W A_1} &= \frac{M_1 / b_W t_S}{A_1 / t_S} \\ &= \frac{M_1 / b_W t_S}{1 + \frac{t_W}{t_S} \frac{b_W}{b_S}} \quad (B2) \end{aligned}$$

With the neutral axis at the center, the value of  $\bar{\sigma}_{\max}$ , which is the stress that must be developed in order to carry the moment, is given by

$$\bar{\sigma}_{\max} = \frac{M_1 / b_W}{\frac{b_S t_S + \frac{1}{6} b_W t_W}{b_S}}$$

which reduces to

$$\bar{\sigma}_{\max} = \frac{M_1 / b_W t_S}{1 + \frac{1}{6} \frac{t_W}{t_S} \frac{b_W}{b_S}} \quad \text{--- (B3)}$$

The value of  $\sigma_{cr}/\eta$  corresponding to  $\sigma_{\max}$  is taken from figure 10 for the material under consideration. The right-hand portion of the curves in figure 10 are obtained from references 3, 5, and 9. (The curve for 24S-T sheet is a lower envelope of the curves of reference 3, and the curves for extruded 75S-T and extruded O-1HTA are an average of the curves of references 5 and 9.) The straight line at the left is simply a plot of the equation  $\bar{\sigma}_{\max} = 1.5\sigma_{cr} = 1.5\frac{\sigma_{cr}}{\eta}$  (for the range covered,  $\sigma_{cr} = \frac{\sigma_{cr}}{\eta}$ ) and is based on the assumption that no buckling of a multiweb wing should be permitted under any flight condition. The design ultimate stress must then never exceed  $1.5\sigma_{cr}$ .

If  $t_W/t_S$  and  $b_W/b_S$  are known, the value of  $k_S$  can be picked from figure 2. Then by transposition of the terms in equation (1),

$$\frac{b_S}{t_S} = \sqrt{\frac{k_S \pi^2 E}{12(1 - \mu^2) \sigma_{cr}/\eta}}$$

and

$$\frac{b_W}{t_S} = \frac{b_W}{b_S} \frac{b_S}{t_S} = \frac{b_W}{b_S} \sqrt{\frac{k_S \pi^2 E}{12(1 - \mu^2) \sigma_{cr}/\eta}} \quad \text{(B4)}$$

The foregoing calculations show the design conditions that apply to a given combination of values of  $t_W/t_S$  and  $b_W/b_S$ . This combination, however, may not be the most efficient way of meeting those design conditions. In order to find the most efficient proportions,  $b_W/b_S$  is varied for each  $t_W/t_S$  to obtain a series of values of  $k_S$ ,  $\sigma_{cr}/\eta$ ,  $b_W/t_S$ , and  $M_1/b_W A_1$  for each value

of  $t_w/t_s$ . Then, for each value of  $t_w/t_s$  (with a given value of  $M_1/b_w t_s$ ), a curve of  $M_1/b_w A_1$  against  $b_w/t_s$  is obtained. The envelope of all these curves shows the maximum efficiency attainable, and the point of tangency of each curve to the envelope shows the value of  $b_w/t_s$  to which each  $t_w/t_s$  corresponds. The point along the individual curve at which it becomes tangent to the envelope indicates the value of  $b_w/b_s$ .

Actually, it was found that, in the elastic range, the value of  $b_w/b_s$  giving maximum efficiency for a given  $t_w/t_s$  was constant (see figs. 3(b), 4(b), 5(b), and 6(b)) and that, above the elastic range, the variation from this value was not appreciable. This single value of  $b_w/b_s$  for each  $t_w/t_s$  was therefore used in the preparation of the charts.

## APPENDIX C

EFFECT OF SHEAR IN THE WEBS ON THE BUCKLING  
STRESS OF MULTIWEB WINGS

The present analysis treats the problem of a multiweb wing in which the buckling of the webs and compression skin under bending loads is of primary significance. Even though the bending loads may be of primary significance, the webs and compression skin will be under a combination of bending and shear loads. The shear stresses in the skin should be low in order to obtain torsional stiffness and thus will be neglected. The interaction of the shear and bending loads in the webs, however, must be considered. The simplest method of considering shear in the webs is by means of an interaction curve so that the approximate effects can be determined.

## Interaction Curve

Figure 11 shows an interaction curve adapted from figure 194 of reference 10. This curve is for a flat rectangular plate simply supported along the edges and subjected to a combination of shear and bending. From reference 10, it appears that the interaction curves are substantially independent of the aspect ratios and the curve given in figure 11 is an average of those given in reference 10.

The shear-stress ratio  $R_s$  is the ratio of the shear stress  $\tau$  actually present in the plate to the critical shear stress of the plate  $\tau_{cr}$  when no other stresses are present. Similarly, the bending stress ratio  $R_b$  is the ratio of the bending stress  $\sigma$  actually present in the plate to the critical bending stress of the plate  $\sigma_{cr}$  when no other stresses are present. Thus, the interaction curve gives the various combinations of bending and shear stress that will cause buckling of the plate.

## Effect of Shearing Stress on Multiweb

## Wing Design

A designer may make a preliminary design of a multiweb wing based on bending loads alone. The shear stress in the webs  $\tau$  and the critical shear stress  $\tau_{cr}$  are then calculated and from

these values the shear-stress ratio  $R_s$  is obtained. The value of the critical shear stress for simply supported edges  $\tau_{cr}$  can be calculated, once the web dimensions and material are known, by the method and charts of reference 14. The value of  $\tau_{cr}$  computed in this manner is probably slightly conservative since the web would be restrained along the upper and lower edges. With the ratio  $R_s$  established, figure 11 can be entered and the ratio  $R_b$  obtained. This ratio  $R_b$  is, then, the ratio of the bending stress  $\sigma$  actually allowable in the web to the critical bending stress  $\sigma_{cr}$  when no other stresses are present. Since  $\sigma_{cr}$  for the preliminary design may be obtained by the use of figure 2, the allowable bending stress  $\sigma$  can be obtained. This stress  $\sigma$ , acting in combination with the shear load, will cause buckling of the wing.

It may be noted from figure 11 that considerable shear can be present without greatly reducing the buckling stress for the webs in bending.

## REFERENCES

1. Kroll, W. D., Fisher, Gordon P., and Heimerl, George J.: Charts for Calculation of the Critical Stress for Local Instability of Columns with I-, Z-, Channel, and Rectangular-Tube Section. NACA ARR No. 3K04, 1943.
2. Boughen, Rolla B., and Baab, George W.: Charts for Calculation of the Critical Compressive Stress for Local Instability of Idealized Web- and T-Stiffened Panels. NACA ARR No. L4E29, 1944.
3. Lundquist, Eugene E., Schuette, Evan H., Heimerl, George J., and Roy, J. Albert: Column and Plate Compressive Strengths of Aircraft Structural Materials. 24S-T Aluminum-Alloy Sheet. NACA ARR No. L5F01, 1945.
4. Heimerl, George J., and Roy, J. Albert: Column and Plate Compressive Strengths of Aircraft Structural Materials. 17S-T Aluminum-Alloy Sheet. NACA ARR No. L5F08, 1945.
5. Heimerl, George J., and Roy, J. Albert: Column and Plate Compressive Strengths of Aircraft Structural Materials. Extruded 75S-T Aluminum Alloy. NACA ARR No. L5F08a, 1945.
6. Heimerl, George J., and Roy, J. Albert: Column and Plate Compressive Strengths of Aircraft Structural Materials. Extruded 24S-T Aluminum Alloy. NACA ARR No. L5F08b, 1945.
7. Heimerl, George J., and Fay, Douglas P.: Column and Plate Compressive Strengths of Aircraft Structural Materials. Extruded R303-T Aluminum Alloy. NACA ARR No. L5H04, 1945.
8. Heimerl, George J., and Niles, Donald E.: Column and Plate Compressive Strengths of Aircraft Structural Materials. Extruded 14S-T Aluminum Alloy. NACA ARR No. L6C19, 1946.
9. Heimerl, George J., and Niles, Donald E.: Column and Plate Compressive Strengths of Aircraft Structural Materials. Extruded O-1HTA Magnesium Alloy. NACA TN No. 1156, 1947.
10. Timoshenko, S.: Theory of Elastic Stability. McGraw-Hill Book Co., Inc., 1936.

11. Budiansky, Bernard, and Hu, Pai C.: The Lagrangian Multiplier Method of Finding Upper and Lower Limits to Critical Stresses of Clamped Plates. NACA TN No. 1103, 1946.
12. Lundquist, Eugene E., Stowell, Elbridge Z., and Schuette, Evan H.: Principles of Moment Distribution Applied to Stability of Structures Composed of Bars or Plates. NACA ARR No. 3K06, 1943.
13. Kroll, W. D.: Tables of Stiffness and Carry-Over Factor for Flat Rectangular Plates under Compression. NACA ARR No. 3K27, 1943.
14. Stowell, Elbridge Z.: Critical Shear Stress of an Infinitely Long Flat Plate with Equal Elastic Restraints Against Rotation along the Parallel Edges. NACA ARR No. 3K12, 1943.

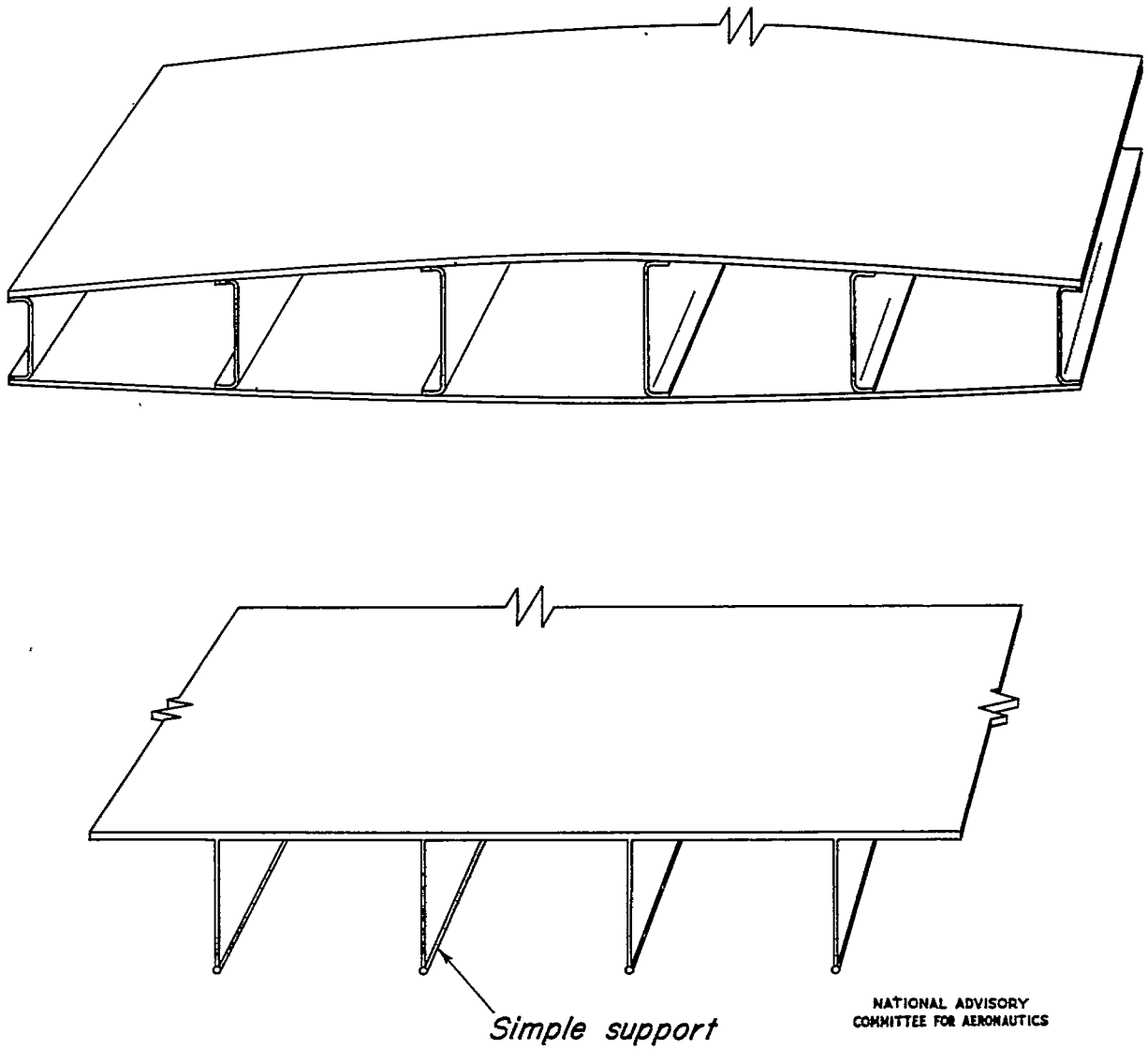
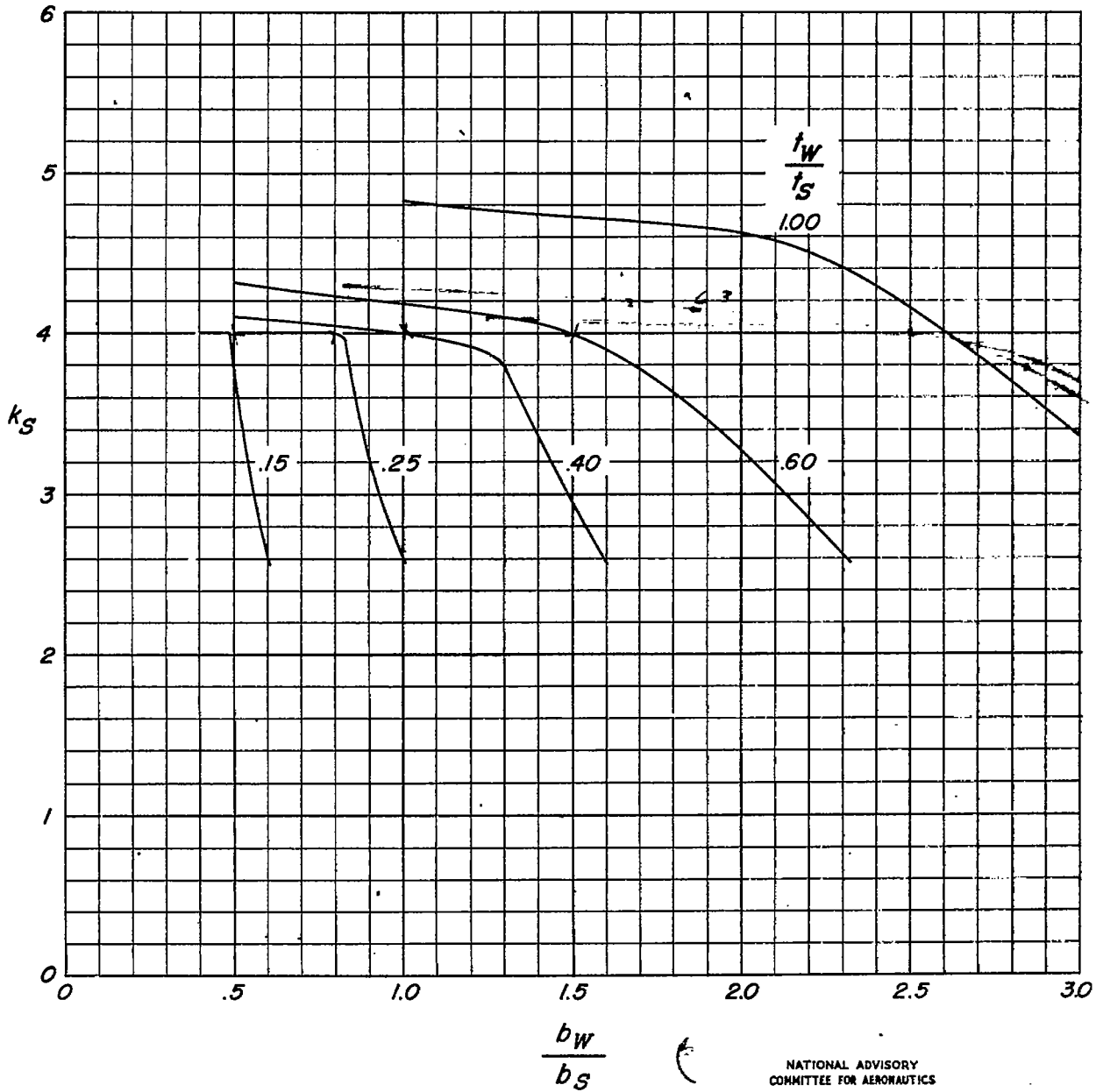
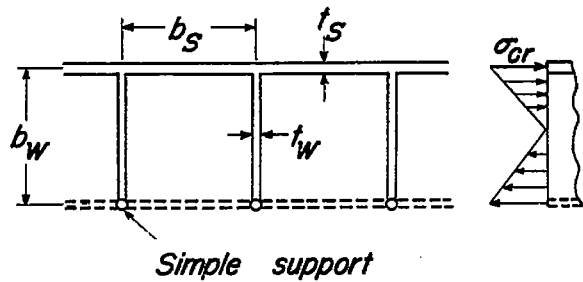


Figure 1.- Multiweb wing and idealized structure.

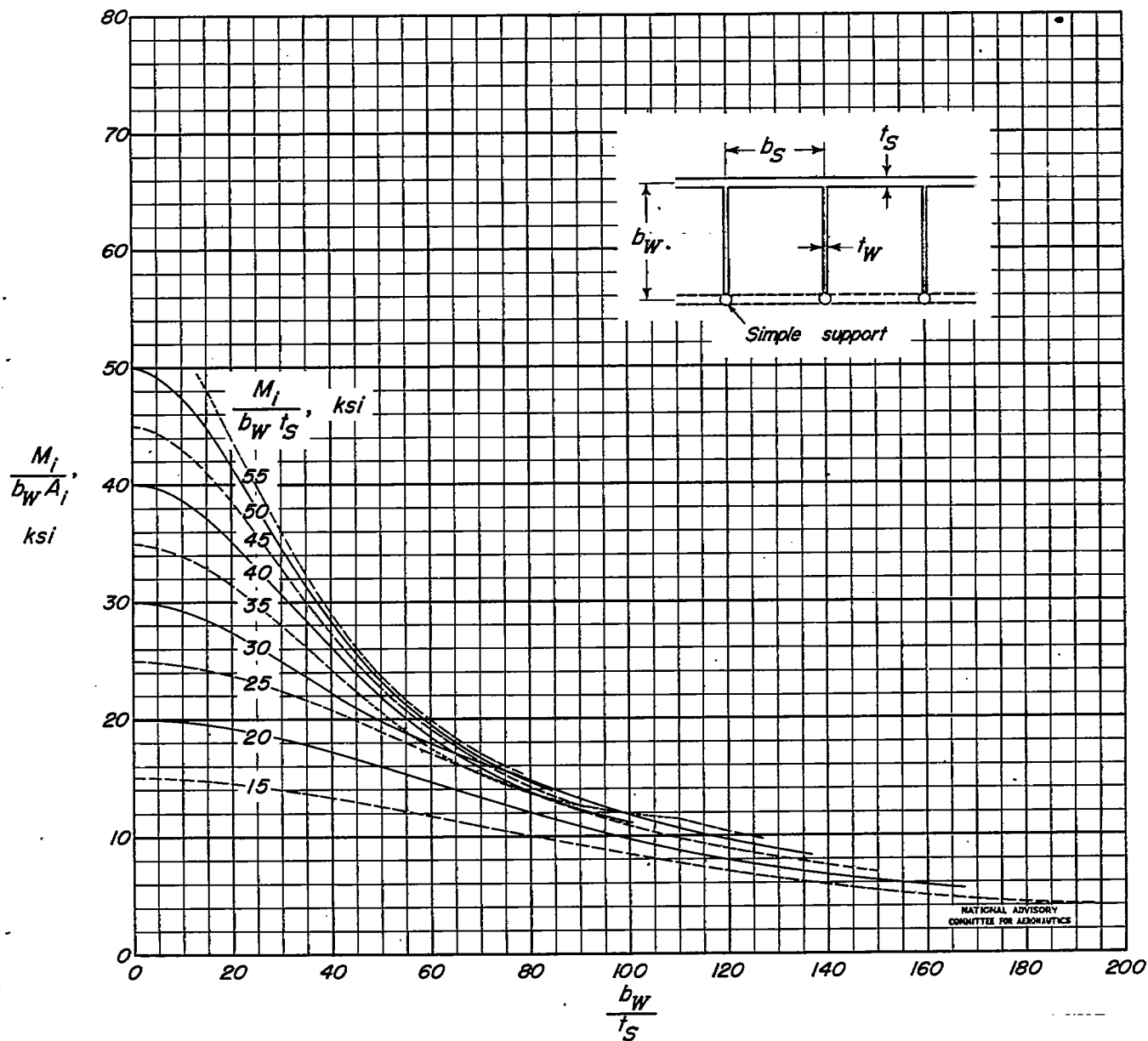


NATIONAL ADVISORY COMMITTEE FOR AERONAUTICS



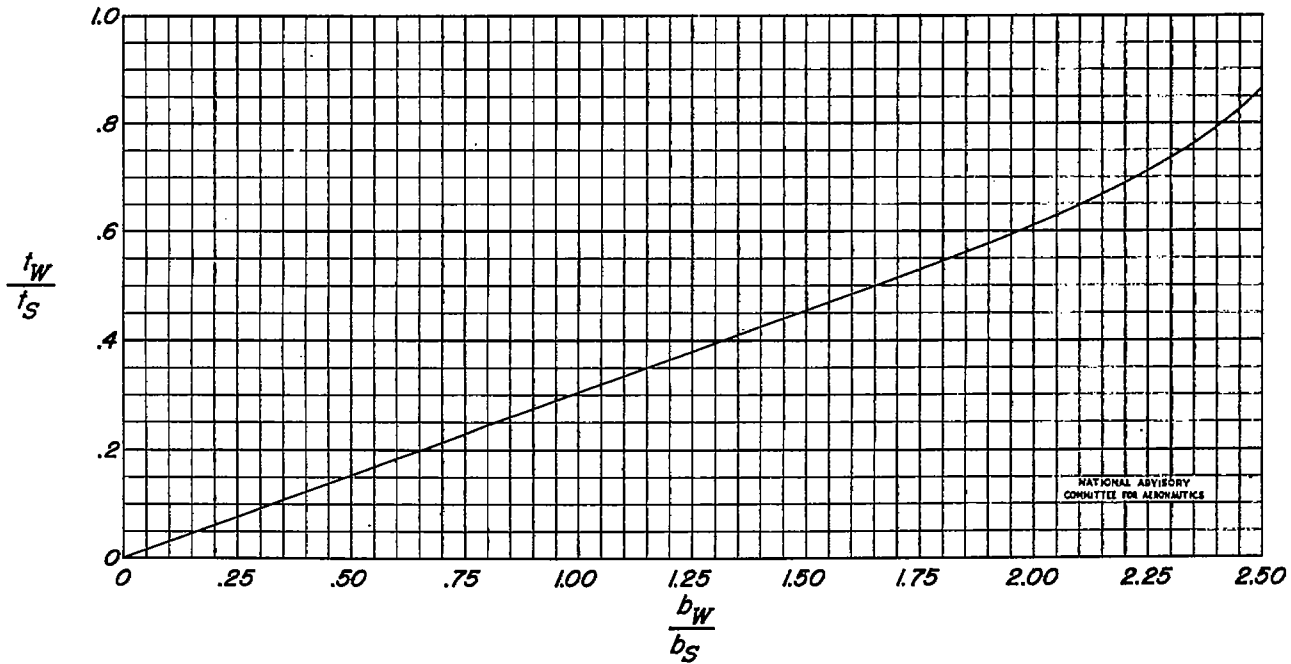
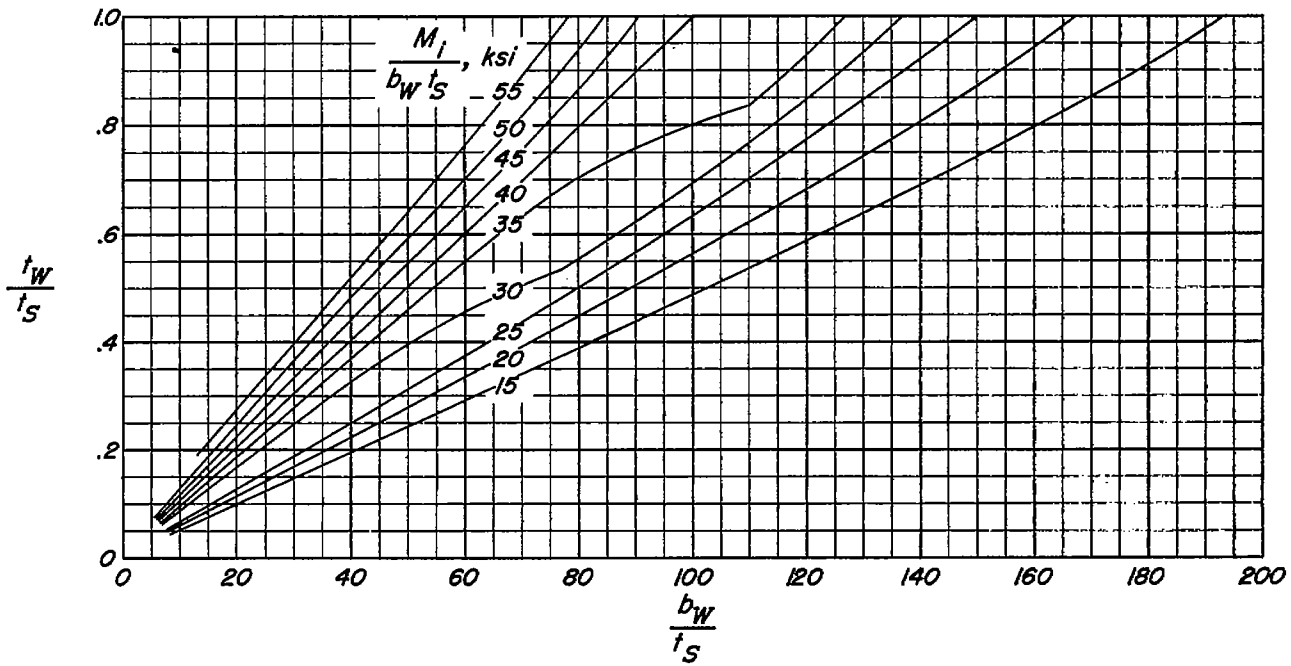
$$\frac{\sigma_{cr}}{\eta} = \frac{k_s \pi^2 E t_s^2}{12(1-\mu^2) b_s^2}$$

Figure 2.- Values of  $k_s$  for idealized multiweb wings in bending.



(a) Values of efficiency parameter  $\frac{M_i}{b_w A_i}$ .

Figure 3.- Design chart for 24S-T aluminum-alloy-sheet multiweb wing.



(b) Dimension ratios for maximum efficiency.

Figure 3.- Concluded.

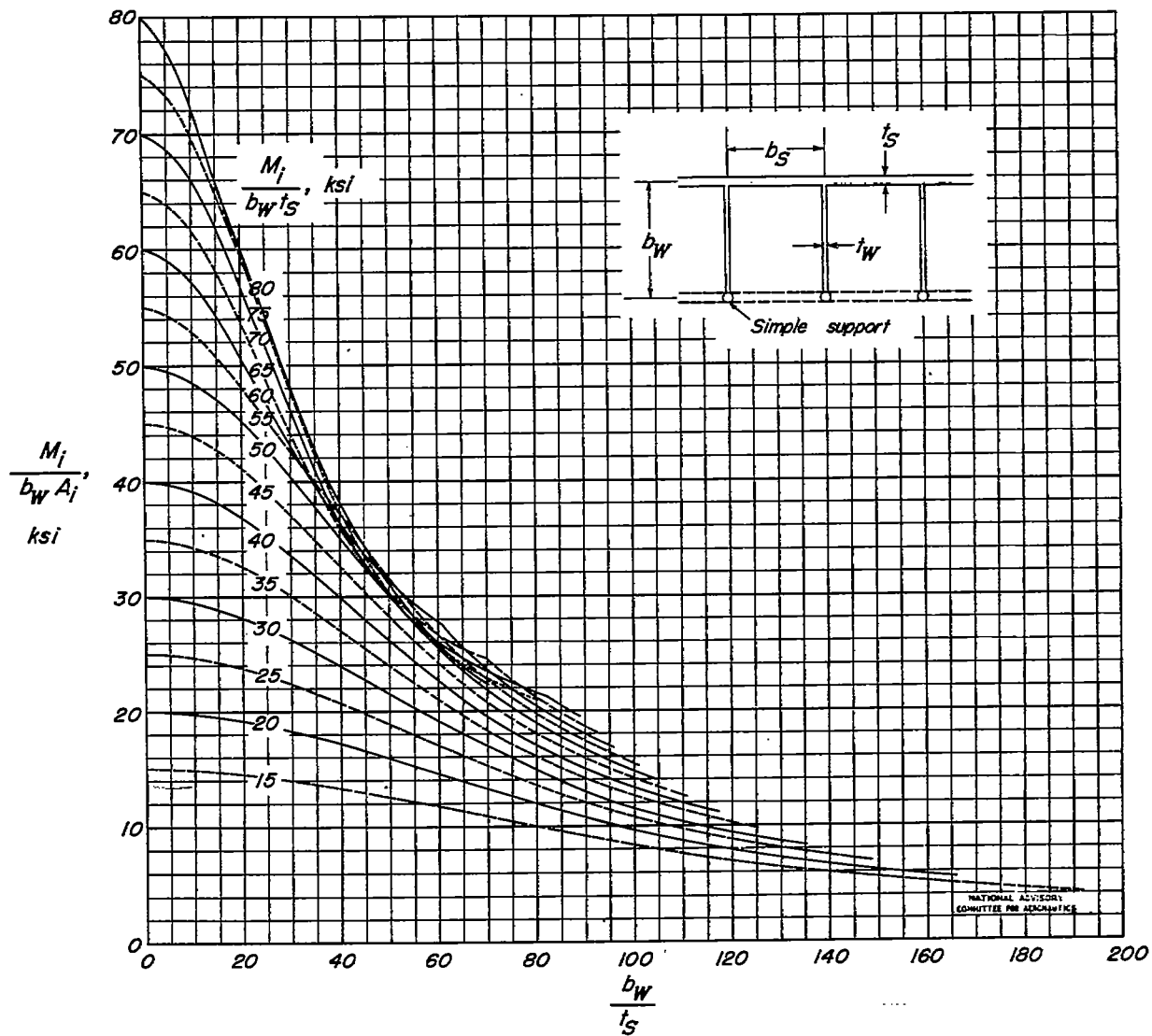
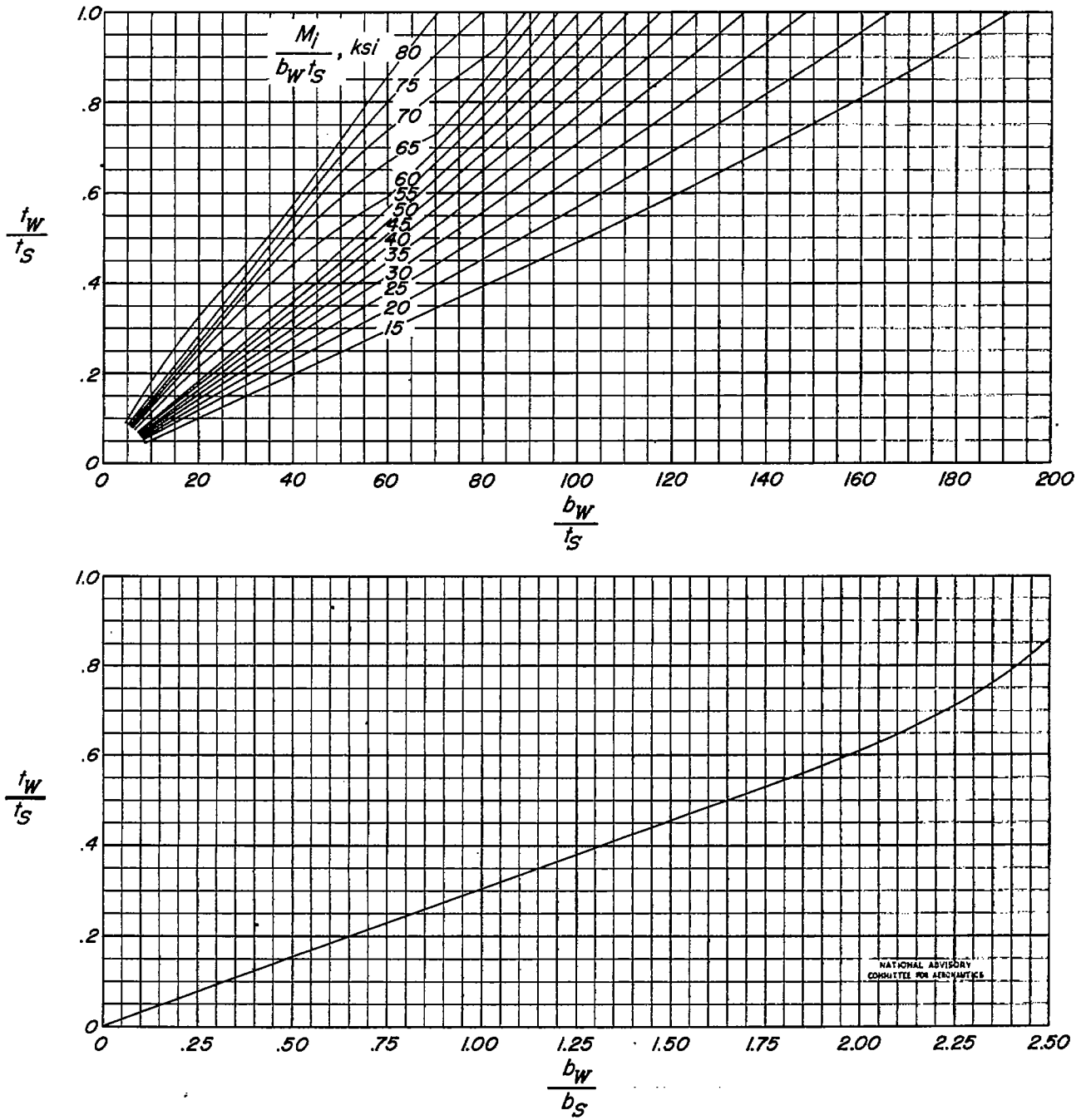
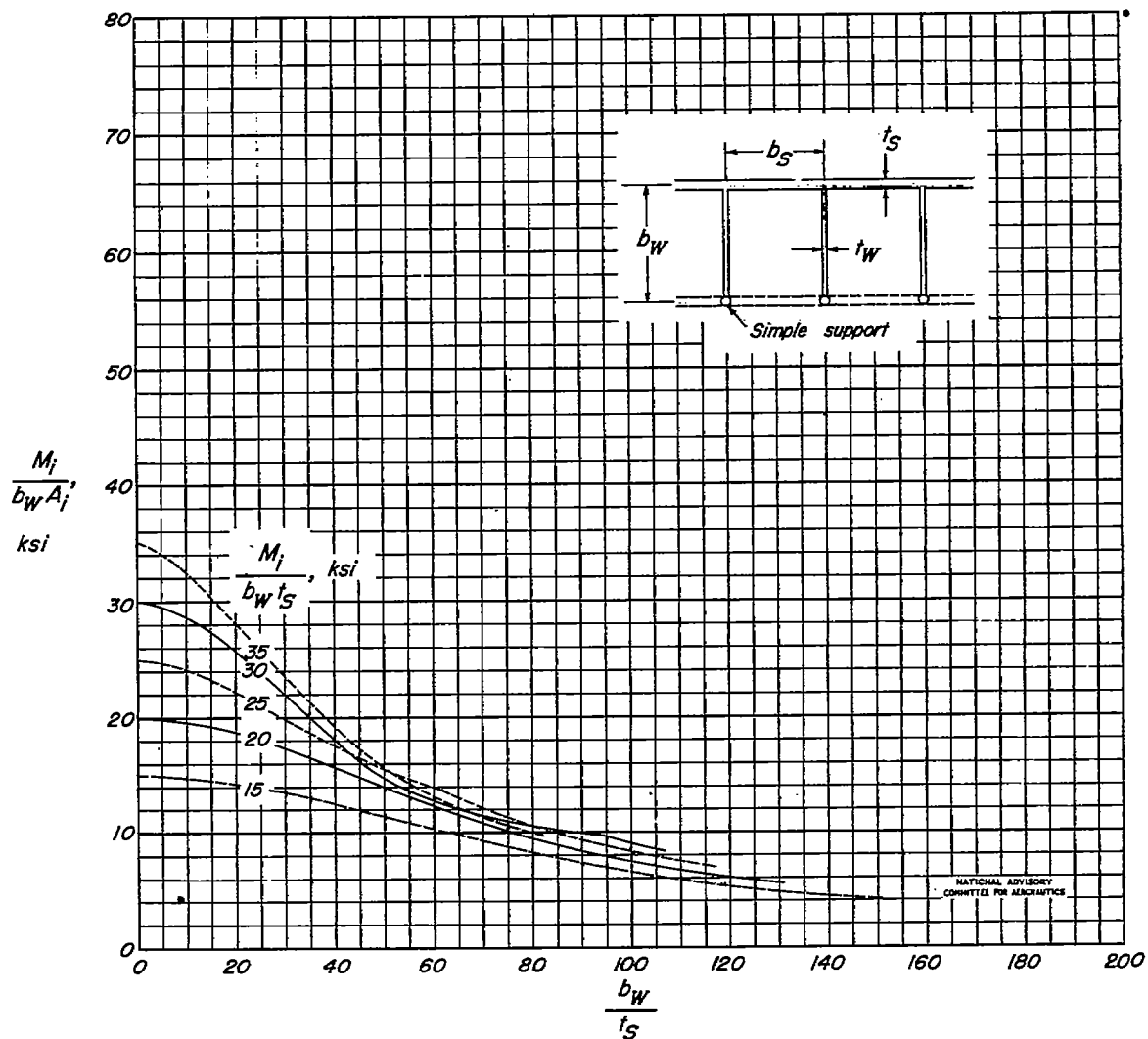


Figure 4.- Design chart for extruded 75S-T aluminum-alloy multiweb wing.



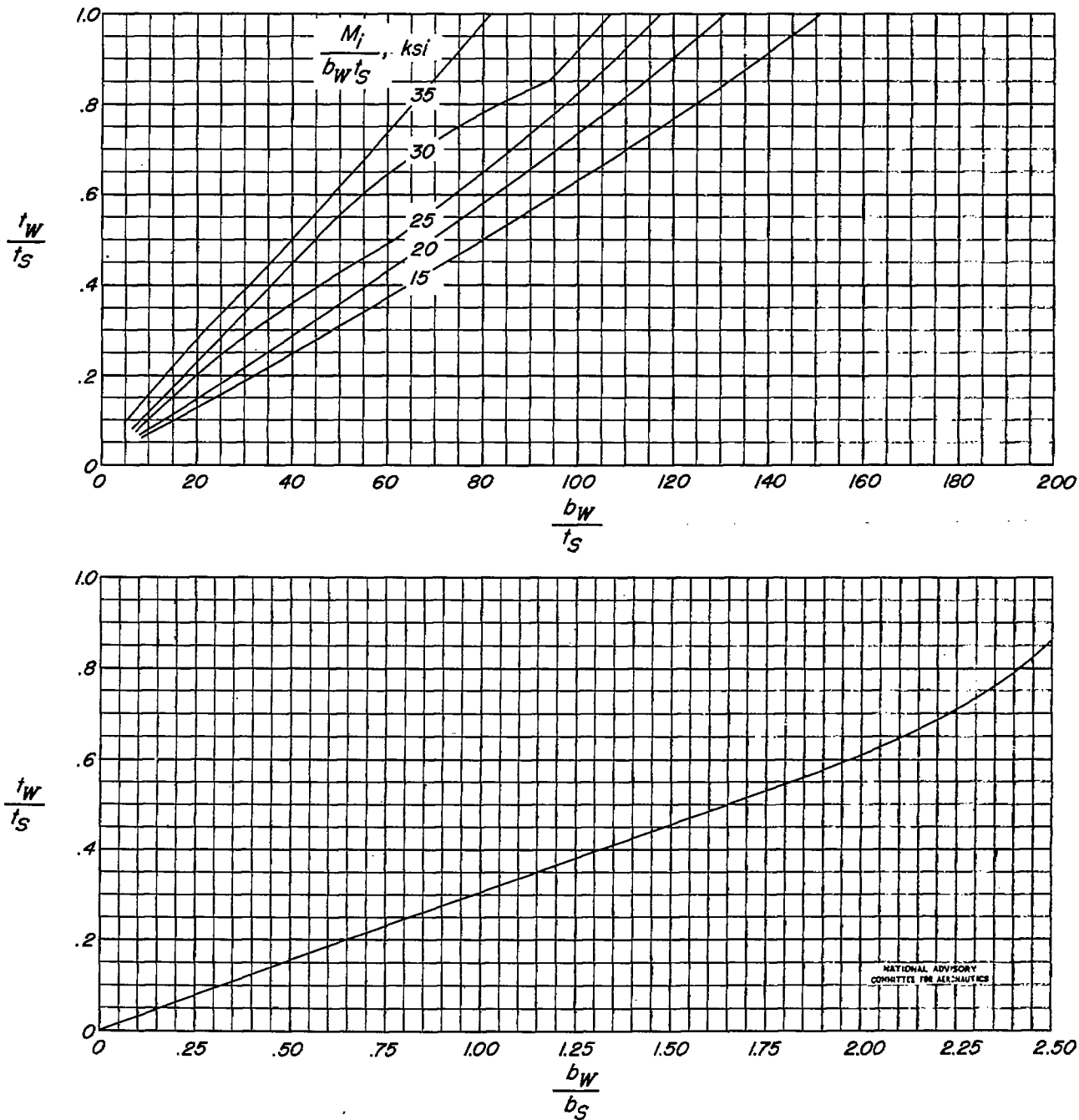
(b) Dimension ratios for maximum efficiency.

Figure 4.- Concluded.



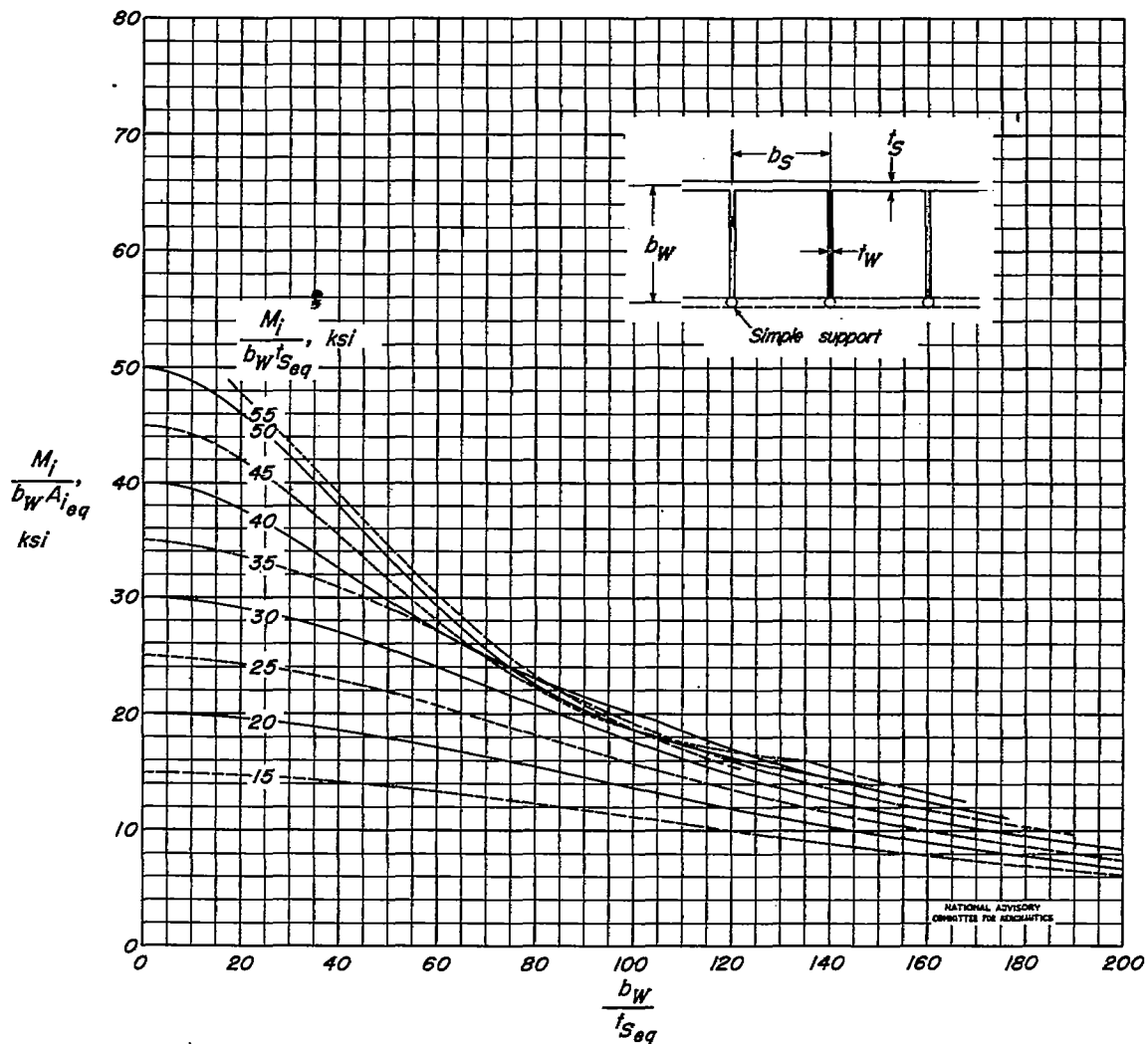
(a) Values of efficiency parameter  $\frac{M_i}{b_w A_i}$ .

Figure 5.- Design chart for extruded 0-1HTA magnesium-alloy multiweb wing.



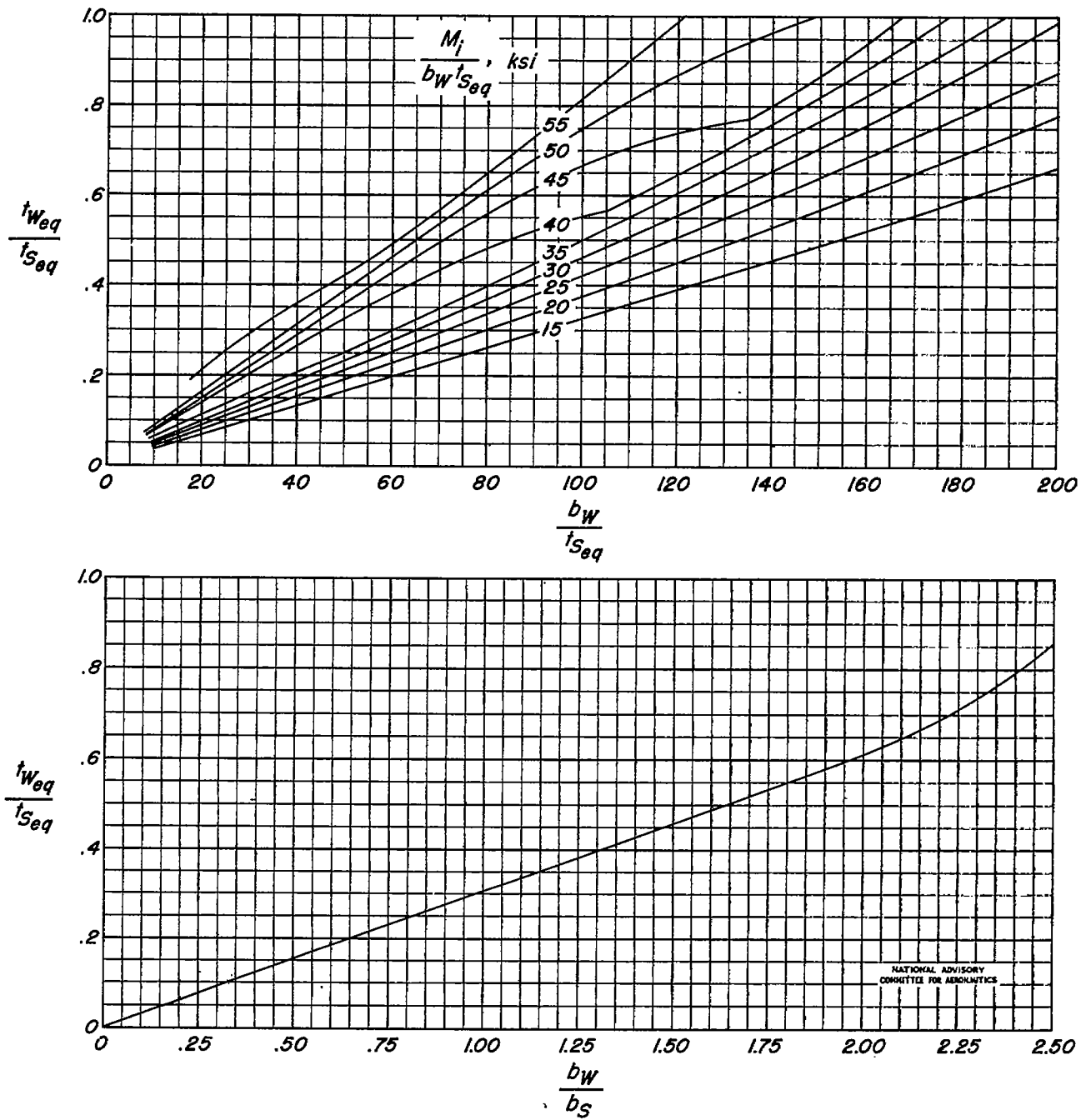
(b) Dimension ratios for maximum efficiency.

Figure 5.- Concluded.



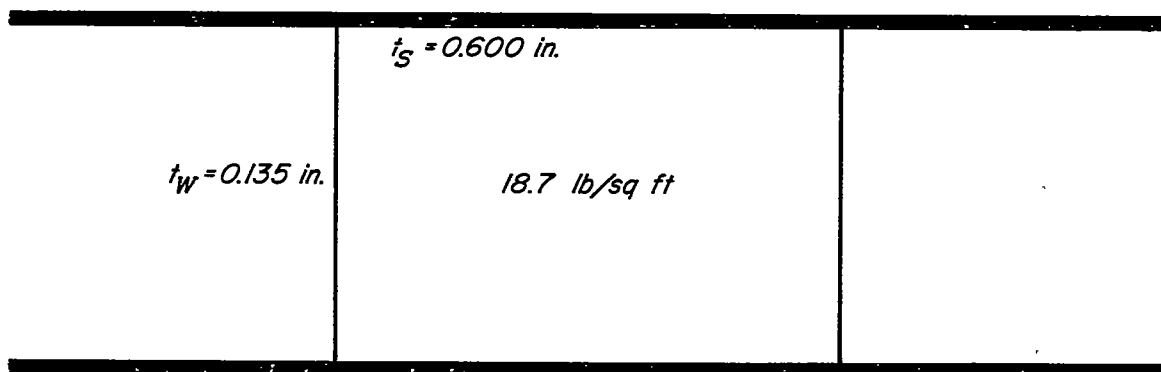
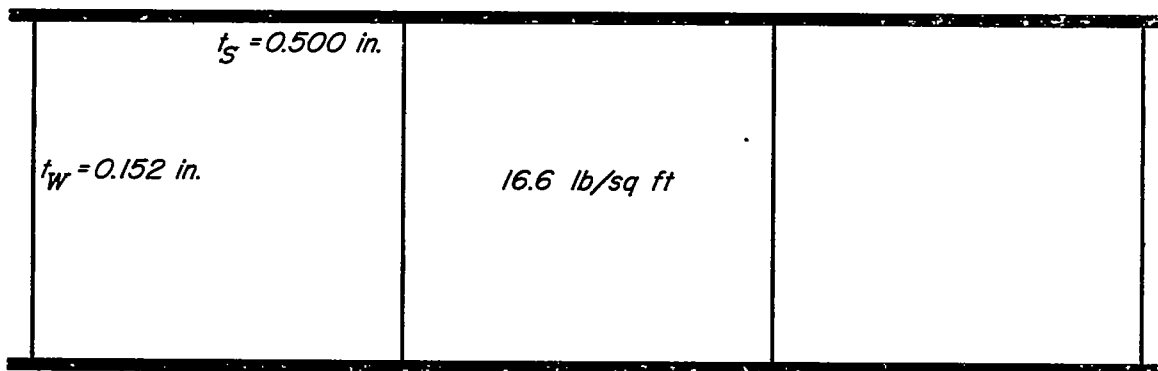
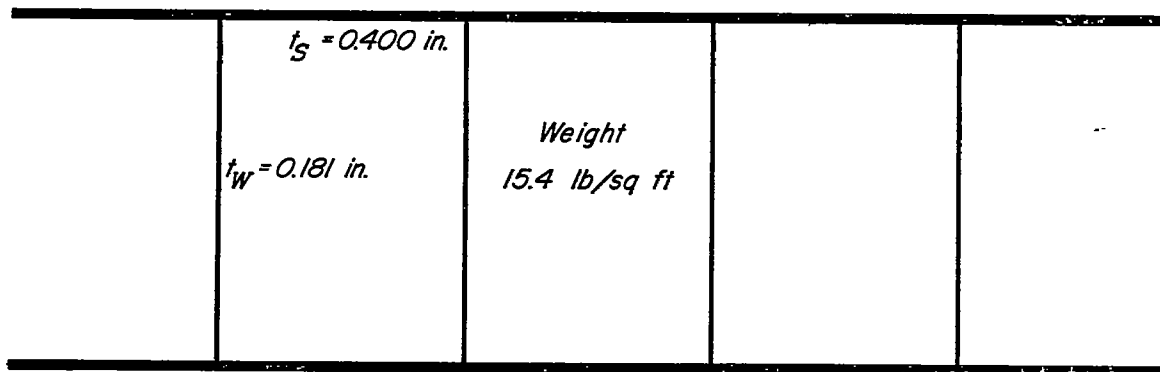
(a) Values of efficiency parameter  $\frac{M_i}{b_w A_{i_{eq}}}$

Figure 6.- Chart for direct weight comparison of extruded 0-1HTA magnesium-alloy with aluminum alloys for multiweb wings.



(b) Dimension ratios for maximum efficiency.

Figure 6.- Concluded.



NATIONAL ADVISORY  
COMMITTEE FOR AERONAUTICS

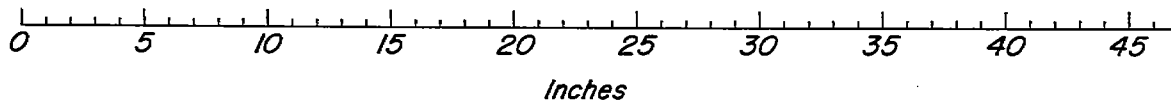


Figure 7.- Cross-sectional views of minimum-weight designs of 24S-T aluminum-alloy multiweb wings with  $M_1 = 300$  inch-kips per inch and  $b_w = 15$  inches.

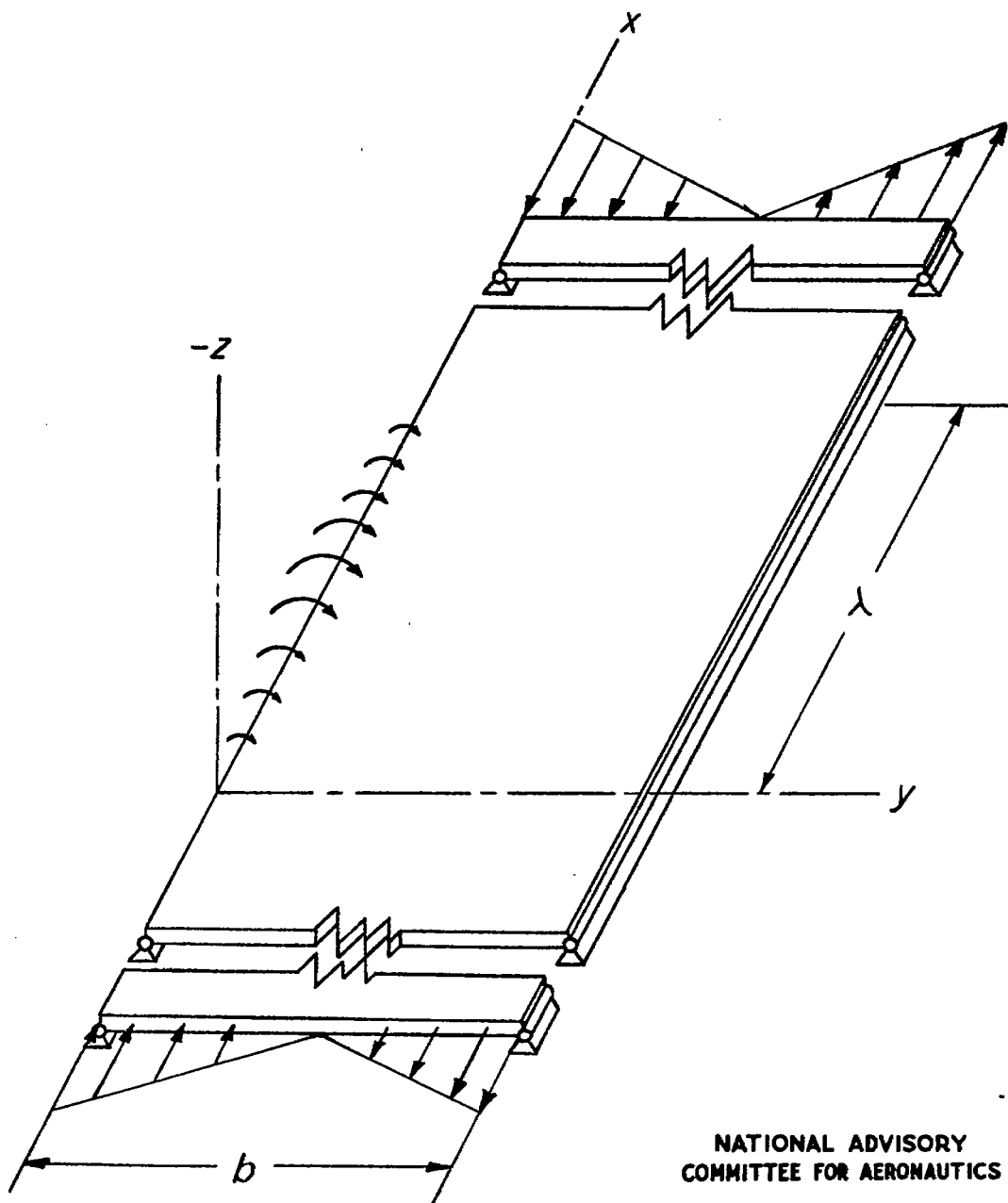


Figure 8.- Infinitely long flat plate under bending forces. Tension edge hinged, compression edge elastically restrained.

*is value for  $\infty$  corner  
No. - Alder's work?*

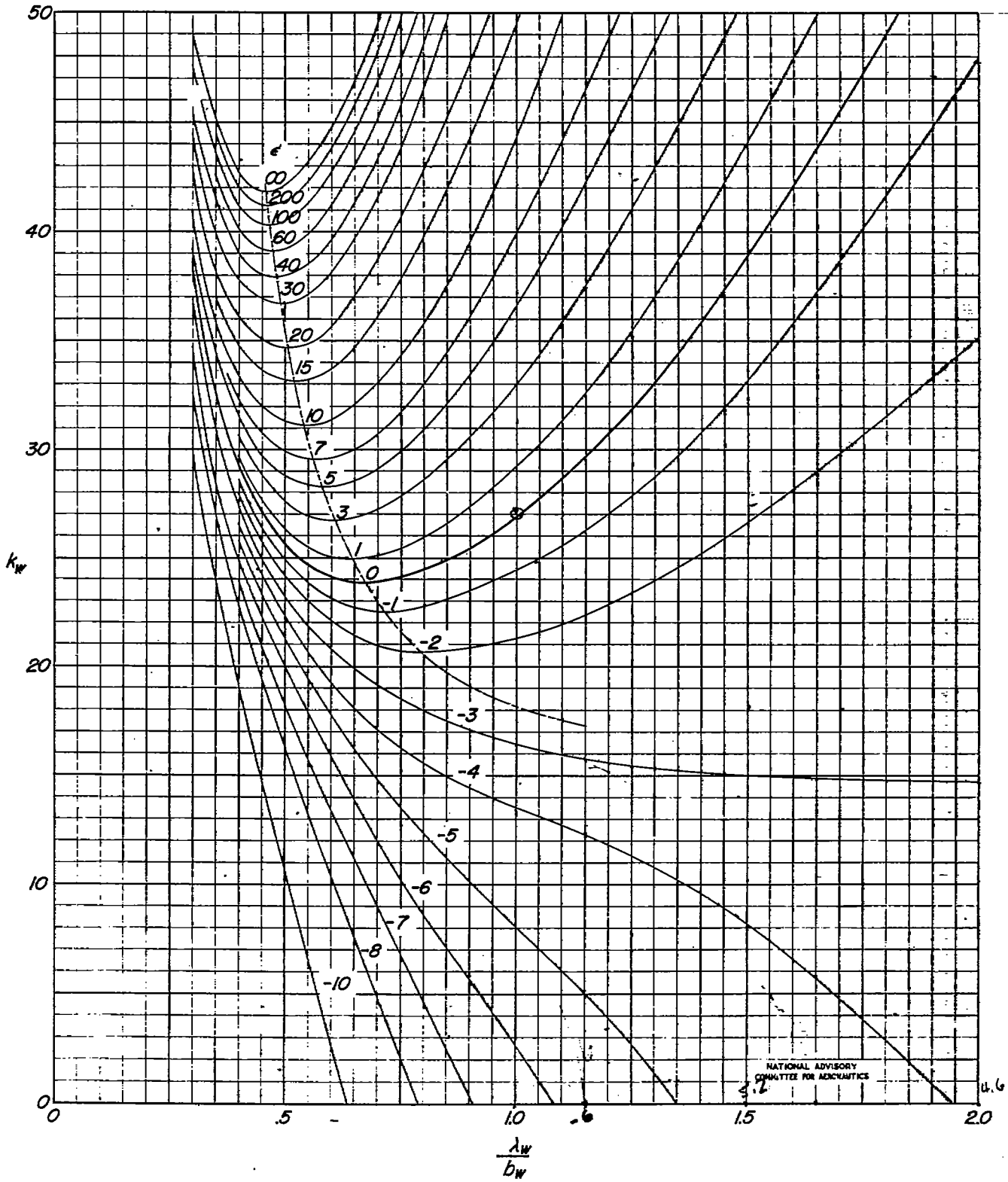


Figure 9.- Values of  $k_w$  for a plate in bending in the plane of the plate with various restraint coefficients  $\epsilon$  along the compression edge.

NATIONAL ADVISORY COMMITTEE FOR AERONAUTICS

4.6

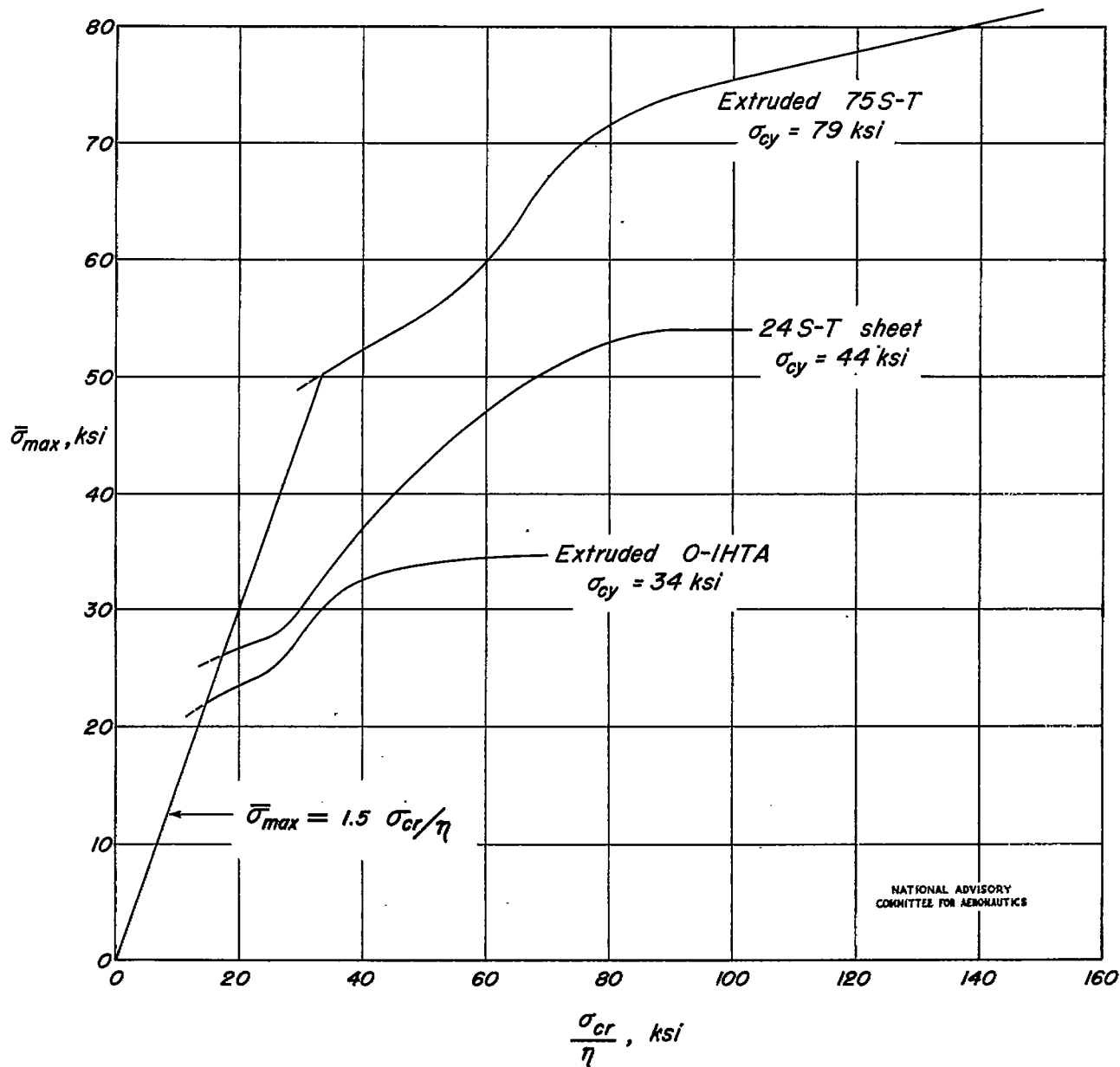


Figure 10.- Variation of  $\bar{\sigma}_{max}$  with  $\frac{\sigma_{cr}}{\eta}$  for extruded 75S-T aluminum alloy, 24S-T aluminum-alloy sheet, and extruded O-1HTA magnesium alloy. (Data from references 3, 5, and 9.)

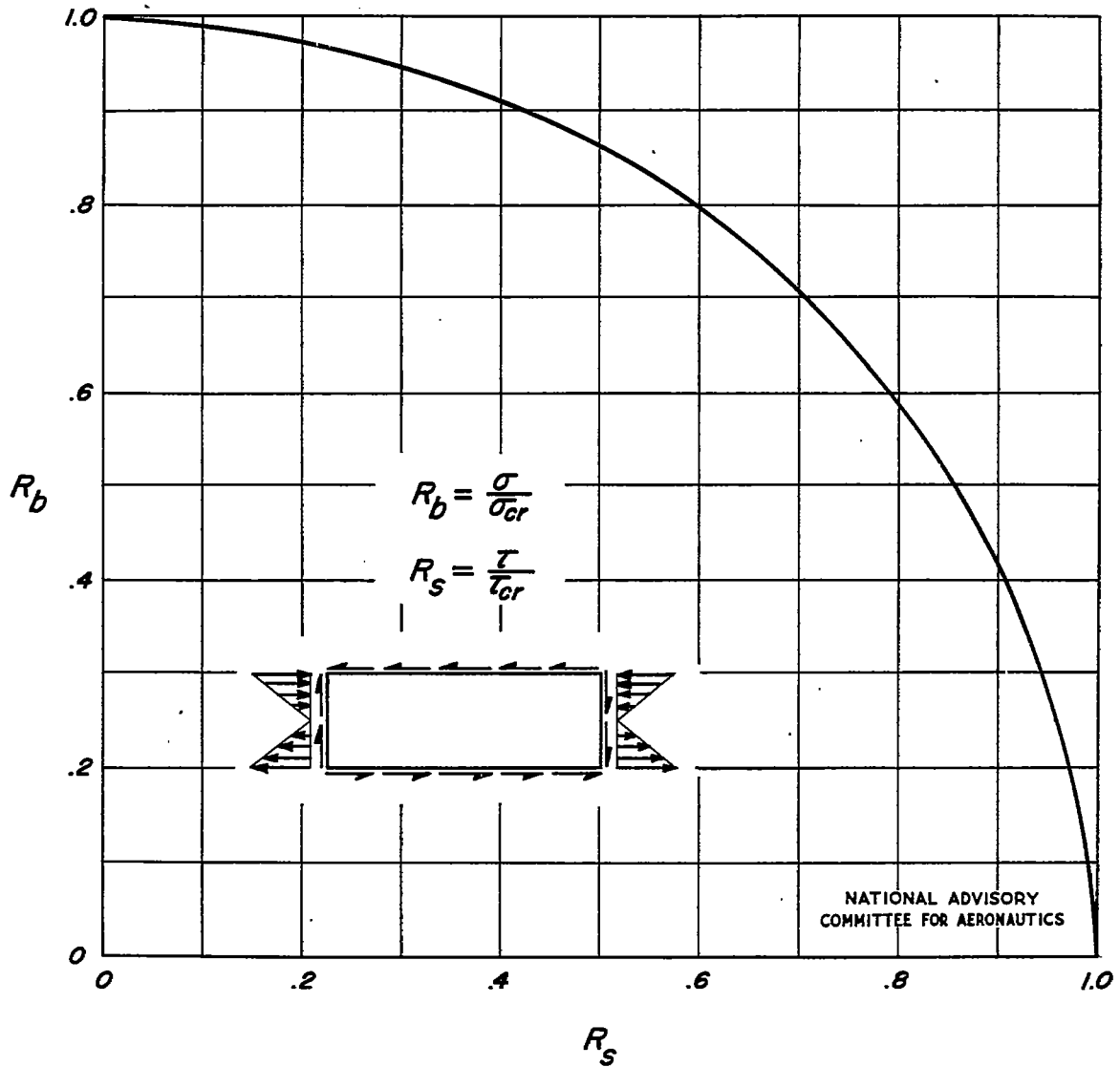


Figure 11.- Interaction curve for plate under bending and shear; edges simply supported. (Average of curves from fig. 194, reference 10.)